Industrial Engineering Journal
ISSN: 0970-2555
Volume : 55, Issue 03 : 2026

TENSILE, COMPRESSION AND SHEAR RESPONSE OF 3D PIERCED FABRIC CARBON- CARBON COMPOSITE

G. Ramaguru, Research Scholar, Department of Mechanical Engineering, University College of Engineering, Osmania University, Hyderabad, Telangana, India.
Dr. K. Saraswathamma, Professor, Department of Mechanical Engineering, University College of Engineering, Osmania University, Hyderabad, Telangana, India.
Atul Ramesh Bhagat, Scientist 'F', Advanced Systems Laboratory, Kanchanbagh, Hyderabad, Telangana, India.

ABSTRACT
Carbon/Carbon (Cf/C) composites have gained significant attention as ultra- high-temperature materials due to their excellent mechanical and thermal properties. These properties can be retained even at temperatures approaching 3000°C. 3D Pierced Fabric (PF) carbon-carbon (Cf/C) composites are particularly attractive for applications subjected to significant flexural loading, such as control surfaces and missile structures. Therefore, understanding their mechanical properties is crucial for evaluating their performance and ensuring structural reliability in high-temperature environments. In this study, the mechanical behaviour of 3D pierced fabric C/C composites was evaluated through tensile, compression, and short beam shear tests at room temperature. The composite exhibited strong anisotropy, with superior tensile stiffness in the X-direction, higher compressive strength in the Z-direction, and an average interlaminar shear strength of 11.74 MPa, demonstrating its suitability for high-temperature structural applications.

Keywords: 3D PF Cf/C composite, tensile, compressive, shear strength

I. Introduction
Carbon-carbon (Cf/C) composites are widely used in aerospace and defence applications, such as nose tips, control surfaces, nozzle throats, brake discs and leading edges due to their exceptional physical and thermal properties, including low density, high specific strength & stiffness and thermal stability at elevated temperatures [1-4]. Normally, Cf/C Composites are made with reinforcement in multi-directional (3D/4D) to orient the carbon fibre with respect to loading directions. For Control-surfaces where bending loads are higher, 3D PF Cf/C composites are chosen with woven Carbon fabric in X & Y directions, resulting in reduced fibre reinforcement through the thickness direction relative to the in-plane directions, thereby contributing to anisotropic mechanical behaviour. Although various reinforcement techniques, including needle-punching, stitching, Z-pinning, and carbon nanotube-grafted carbon fibres, have been used to enhance interlaminar shear (ILS) strength, it remains lower than the strength in other directions [5,6]. Carbon fibre pultruded rods are inserted in the Carbon Fabric stack in 3D PF Carbon preforms to improve through thickness properties. Moreover, the carbon matrix in the interlaminar region has relatively low shear strength, making Cf/C composites prone to ILSS failure. These failures can reduce the tensile and compressive performance of the composites and negatively affect the reliability of the structure. Therefore, studying the interlaminar shear behaviour and failure mechanisms of 3D PF Cf/C composites is essential for improving their structural performance and reliability [7].
Unlike conventional 3D woven, braided, or needle Cf/C composites, 3D pierced fabric (3D PF)-based Cf/C composites are fabricated by reinforcing stacked carbon fabric layers with through-thickness fibre bundles/rods introduced through a piercing process. This unique architecture enhances the interlaminar bonding between layers and improves resistance to delamination and interlaminar shear failure. Since the mechanical response of these composites is highly dependent on their reinforcement

architecture, accurate characterisation of their properties is necessary for assessing their structural performance and reliability.

Guo et al. [1] reported that, under quasi-static loading, the pierced fibre bundles fail primarily by tensile rupture, leading to interlaminar shear (ILS) failure in three-dimensional fine weave pierced carbon/carbon (3D FW PF Cf/C) composite. In contrast, under high strain-rate loading shear fracture of the pierced fibre bundled becomes the dominant failure mechanism. Ramaguru et al. [8] demonstrated that mechanical properties of the 3D PF Cf/C composite are significantly influenced by material anisotropy. Their study showed that the through-thickness (z-direction) behaviour differed considerably from the in-plane directions.

Li et al. [9] revealed that compression strength and stiffness of 3D needle- punched Cf/C composites decrease with increasing temperature because of oxidation-induced degradation. Their study further demonstrated that the reinforcement architecture and fibre-matrix interfacial integrity have critical influence on mechanical performance on the high temperature mechanical performance of the composites. Zhong et al. [10] reported that the preform architecture of 3D orthogonal woven Cf/C composites significantly affects the pore distribution, graphitisation degree, and overall composite performance.

Aly-Hasan et al. [7] compared the damage and fracture resistance of 2D and 3D Cf/C composites. They reported that 3D Cf/C composites exhibited weaker interfaces due to higher residual stresses caused by the constraints imposed by the three-dimensional fiber architecture. Davies and Rawlings [11] investigated the compressive properties of 2D Cf/C composites fabricated using the chemical vapor infiltration (CVI) technique and compared them with non-CVI composites. Their results showed that CVI composites possessed better in-plane compressive properties but lower out-of-plane compressive properties for similar densities. Adams [12] performed a microstructural analysis of 3D reinforced Cf/C composites and examined the evolution of mechanical properties during processing. The study revealed that interface debonding, resulting from thermal expansion mismatch between the anisotropic carbon fibers and the matrix, along with the constraints of the 3D fiber architecture, significantly influenced material degradation. Bhagat and Mahajan [13] characterized the carbon matrix produced through pitch impregnation and found that the pitch-derived carbon matrix exhibited plastic deformation behavior accompanied by damage accumulation.

Overall, the literature demonstrates that the mechanical behavior and failure mechanisms of 3D C/C composites are highly dependent on their reinforcement architecture. While needle-punched and orthogonal woven composites have been extensively studied, limited information is available on the tensile, compressive and shear behavior of 3D pierced fabric Cf/C composites. Therefore, a detailed investigation of the tensile, compression, and shear properties of 3D PF Cf/C composites is necessary to better understand their structural performance and support their application in demanding thermo-structural environments.

II. Composite Fabrication

A 3D PF Cf/C composite was fabricated using the standard Cf/C composite fabrication process available at the Lab. The 3D reinforcement structure, which acts as the primary load-bearing member of the composite, is referred to as the preform. The fabricated composite was a 3D-pierced fabric-type Cf/C composite. The reinforcement was provided in two forms: 8H satin-weave carbon fabric (Fig. 1) laid up in the fixture and carbon epoxy pultruded rods of Ø 2mm (Fig. 1) inserted through the thickness direction. PAN-based Toray fill-grade carbon fibre was used for the fabrication of both the fabric and pultruded rods. The epoxy resin used for fabricating the pultruded rod was Lapox L-12, and the hardener used was Lapox K-6, supplied by M/s Atul Ltd, India. The curing temperature employed during the pultrusion was 130°C. The smooth surface achieved during pultrusion results in weaker adhesion to the carbon matrix compared to the carbon fibre tows, which possess rough, uneven surface textures. The rough surface texture facilitates better bonding between the fibre and the matrix compared to the smooth surface in circular rods.

The carbon fabric provides reinforcement in the XY directions, whereas the inserted carbon fibre rods provide reinforcement in Z-direction. The skeleton of the reinforcement (preform) possesses fibre volume fractions of 25% in the X and Y directions, and 5% in Z direction. This kind of preforms are characterized by high in-plane reinforcement with sufficient through thickness reinforcement to avoid delamination. These preforms are typically used in structures like control surfaces subjected predominantly to bending loads during flight conditions. For the present study, preforms were fabricated as per the characterization tests and for conducting machining studies. Fig.2 illustrates the preform unit cell for 3D pierced fabric architecture. It shows the fibres in X and Y directions (warp and weft) along with Z-direction circular rods. Fig.3 illustrates the the fabricated 3D PF C/C composite preform with Z-direction reinforcement.

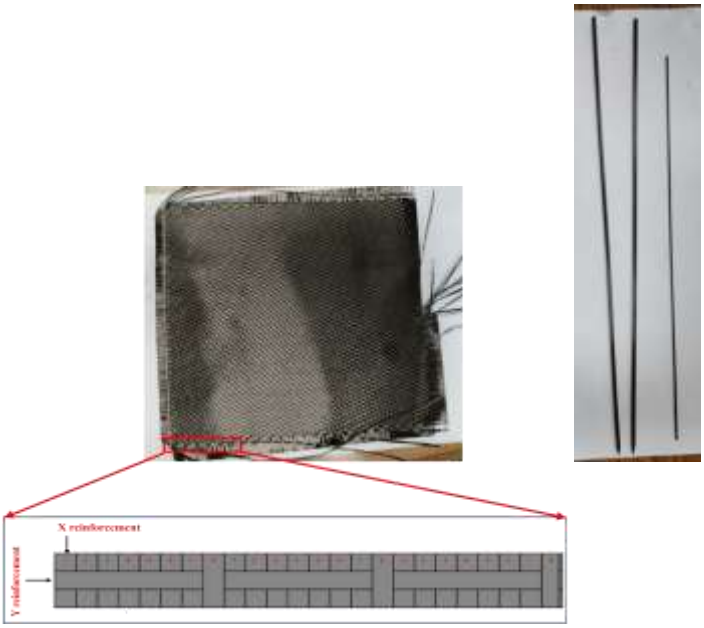

Fig. 1: 8H Stain fabric and carbon-epoxy pultruded rods (Z-Direction Reinforcement)

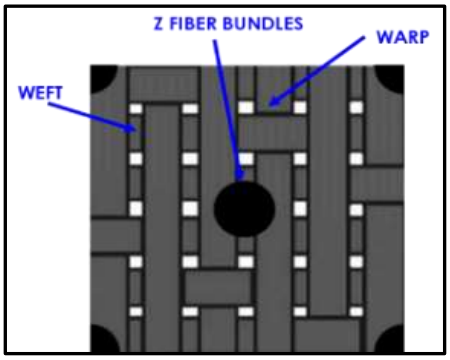

Fig. 2: Preform unit cell for 3D pierced fabric architecture

Fig. 3: 3D Pierced Fabric (8H Satin Weave) Preform

The densification cycles involving impregnation, high-pressure impregnation, carbonization, and graphitization were repeated until the required density was achieved. Table 1 summarizes the reinforcement architecture, matrix details, fibre volume fractions, and fabrication parameters of the composite. Table 2 presents the properties of the reinforcement material used for composite fabrication. Fig. 3 shows the fabricated 3D PF C/C composite, while Fig. 4 shows the microscopic image of the composite. Specimens of the required dimensions were prepared from the main billet for further analysis, and the samples prepared for machining studies are shown in Fig. 5.

Table 1: 3D PF C/C elements and their process parameters

The type of Principal reinforcement	The type of Matrix	Production process	HTT [°C]	Density [kg/m3]	Fiber volume fraction [%)]		
					Vfx	Vfy	Vf z
PAN-based T-300 carbon fabric	Coal tar pitch-based carbon	Liquid Impregnation Technique	>2200°C	1920	25.0	25.0	5.0

Table 2: Properties of carbon fabric used in composite fabrication

Major reinforcement	Type of weave	Carbon content [%]	Thickness [mm]	Tensile strength [N/m]
PAN based T-300 carbon fabric	8H Satin weave	92	0.35	69496

Industrial Engineering Journal
ISSN: 0970-2555
Volume : 55, Issue 03 : 2026

Fig.3: Fabricated 3D PF C/C composite billet

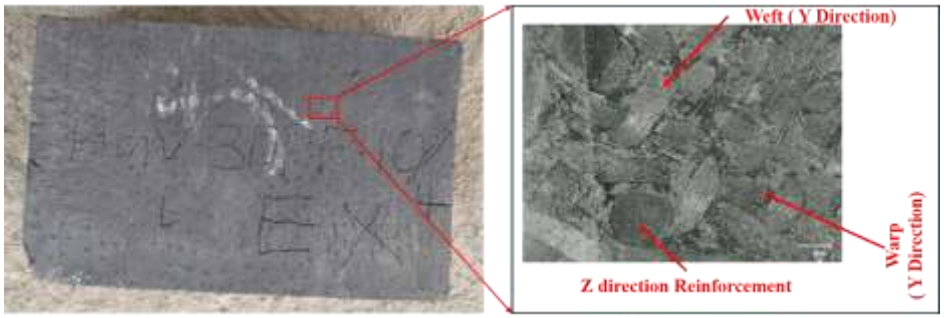

Fig. 4: Microscopic image of 3D PF C/C composite

Fig.5: Samples prepared for experimentation

Two specimens were extracted from the fabricated 3D pierced fabric carbon/carbon (3D PF Cf/C) composite for micro-computed tomography (micro-CT) analysis. Micro-CT is a non-destructive evaluation technique used to examine the internal integrity and defect distribution within composite materials without damaging the specimens.

The reconstructed micro-CT slice images and 3D rendered views are shown in Fig.6 and Fig.7. Both specimens exhibited a dense, uniform internal structure throughout the scanned volume. No significant internal defects such as voids, cracks, delamination, or inclusions were observed in the analysed regions. The absence of such defects indicates good densification and proper fabrication quality of the 3D PF Cf/C composite.

Based on the micro-CT results, the fabricated specimens meet the industry acceptance requirements, confirming that the composite has defect-free internal structural integrity suitable for further mechanical and machining investigations.

Industrial Engineering Journal
ISSN: 0970-2555
Volume : 55, Issue 03 : 2026

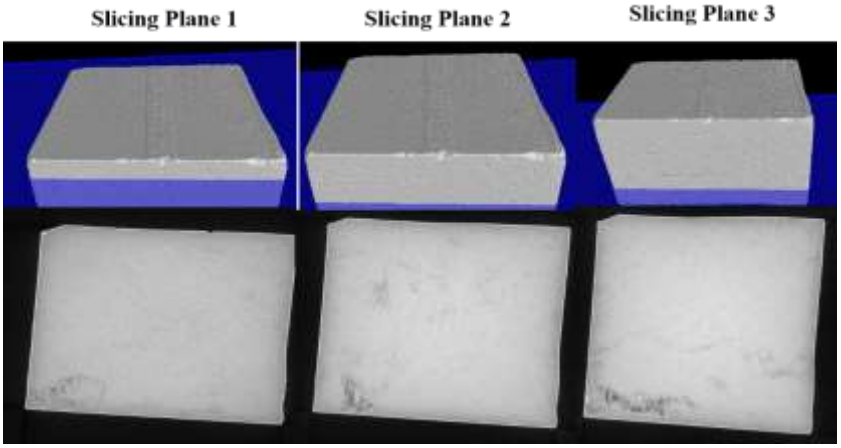

Fig 6: Specimen 1 Micro-CT slices and 3D Constructed models

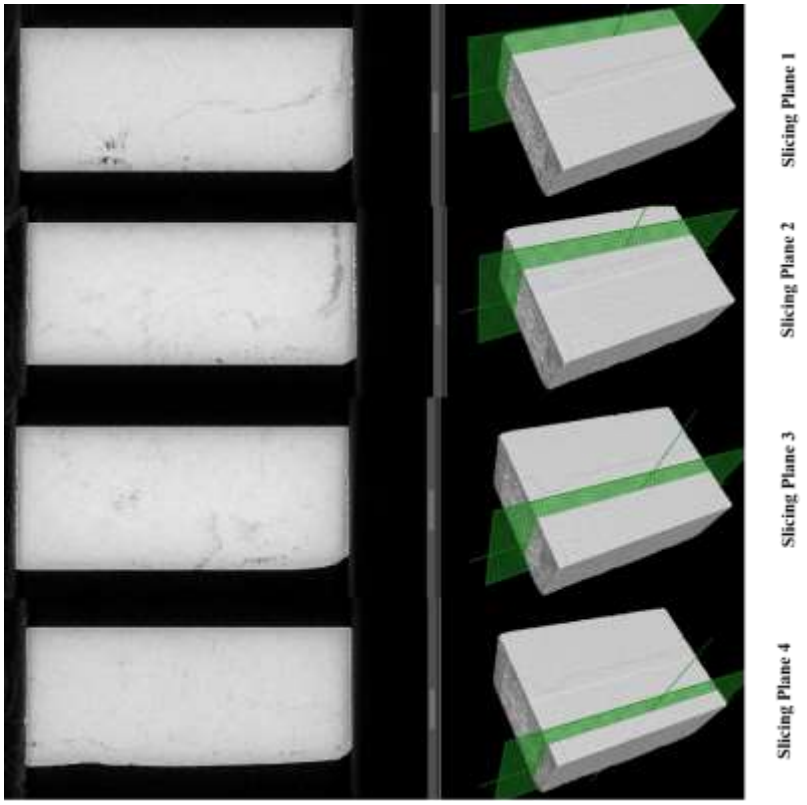

Fig. 7: Specimen 2 Micro-CT slices and 3D Constructed models

III. Specimen preparation, Test equipment, and test methodology

This section describes the shear, compression, and tensile tests performed on the composite at room temperature using a Universal Testing Machine (UTM). The test specimens were machined according to standard specifications. Extensometers and strain gauges were employed to measure the strain during testing. The following sections provide a detailed explanation of each test.

3.1 Short beam shear test

Short beam shear (SBS) tests were carried out to evaluate the shear strength of the 3D PF Cf/C composite. Although this test cannot be used to determine the shear modulus, it is widely employed for the rapid assessment of shear strength, particularly the interlaminar shear strength of composite materials. The 3D Cf/C composite specimens were machined to dimensions of 100 x 13 x 11 mm as

per the standard ASTM D 2344, and their geometry is shown in Fig.8. A total of four specimens were machined and tested. All specimens were extracted from the X-Y plane of the composite.

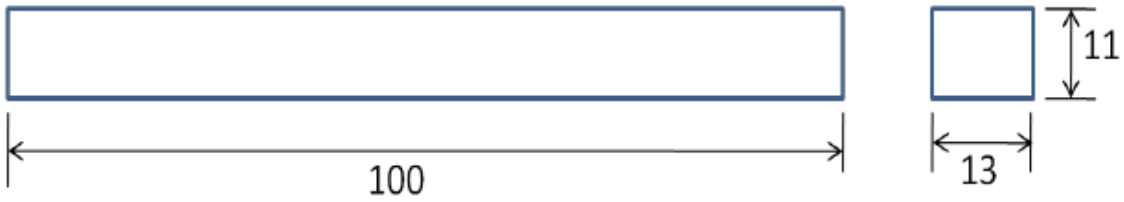

Fig.8: SBS test specimen

The SBS tests were performed using a universal test machine (UTM) (Fig. 9). The support span length was maintained at 45mm, and the tests were carried out at a crosshead speed of three -point bending fixtures commonly employed for flexural testing. The resulting span-to-depth ratio was 3.46. A relatively small span-to-depth ratio is necessary to promote shear failure within the specimen rather than tensile or compressive failure. This differs from conventional flexural testing, which typically employs a span-to-depth ratio of 16:1 to minimise the influence of shear stresses on specimen failure.

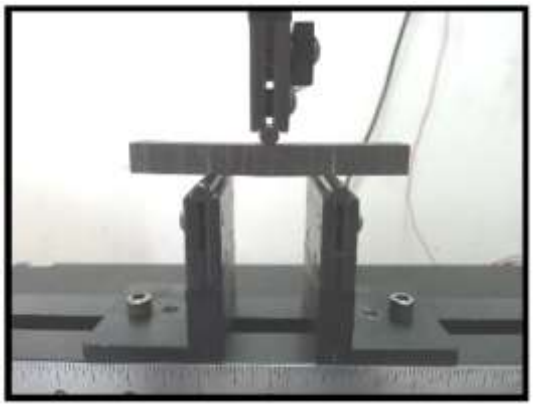

Fig.9: SBS test set up

3.2 Compression test

The specimen dimensions for the compression test were 12 × 12 × 24 mm, as specified by ASTM D695. Specimens were equipped with strain gauges to monitor strain during the test. Fig 10(a) and (b) show the compression test specimen and the test setup. These compression tests were done at a speed of 0.5 mm/min.

Fig. 10 (a): Compression test set-up

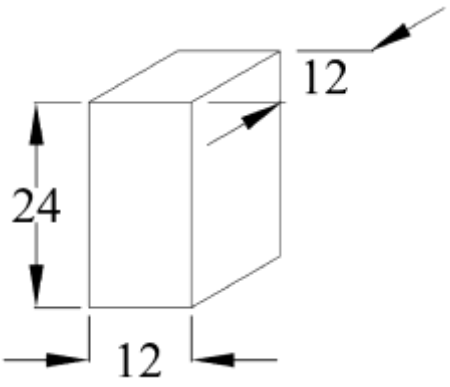

Fig. 10 (b): Compression test specimen

Industrial Engineering Journal
ISSN: 0970-2555
Volume : 55, Issue 03 : 2026

3.3 Tension test

Tensile tests were conducted using double-contoured dog-bone shaped specimens. The double-contour geometry was incorporated to facilitate secure gripping of the specimens during high-temperature testing. Fig. 11 illustrates the geometry of the tensile test specimen with double contour ends. Stainless steel gripping fixtures were used to clamp the specimens during testing. The contoured profile enhanced the grip and minimised the possibility of specimen slippage ensuring reliable load transfer throughout the test.

The tensile tests were performed at room temperature. The mechanical properties determined from these tests included tensile strength, elastic modulus, and failure strain. The specimen geometry had a gauge length of 20 mm and a gauge cross-sectional area of 10 mm x 12 mm. The specimen geometry was designed to ensure failure within the gauge section while maintaining stable gripping under ambient testing conditions. Table 3 summarizes the parameters obtained from the tensile test and compression tests performed at room and elevated temperatures.

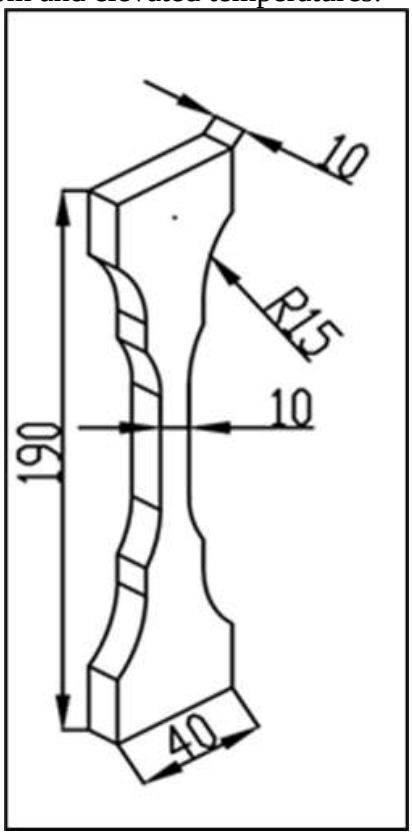

Fig. 11: Tensile test specimen

Table 3: Test methods and parameters extracted

Test Method	Parameters determined
Tension X, Z	E_{Tx} , E_{Tz} , σ_{Tx} , σ_{Tz}
Compression X, Z	E_{Cx} , E_{Cz} , σ_{Cx} , σ_{Cz}

IV. Results and discussion

Industrial Engineering Journal
ISSN: 0970-2555
Volume : 55, Issue 03 : 2026

4.1 The results of the SBS test

Fig.12 shows the load-displacement curve obtained from the SBS tests. The SBS strength was calculated in accordance with ASTM D 2344 using the following equation:

$$SBS = \frac{3P}{4bh} - - - - - - - - - - - - - - - - - - (1)$$

Where P is the maximum load, b and h are the width and height of the specimen respectively.

It can be observed that all the load-displacement curves exhibit consistent behaviour in terms of slope and failure characteristics. The specimens failed gradually rather than suddenly, demonstrating the composite's typical progressive failure behaviour. The SBS strength results determined for four specimens are given in Table 4. The average short beam shear strength was found to be 11.74 ± 1.29 MPa.

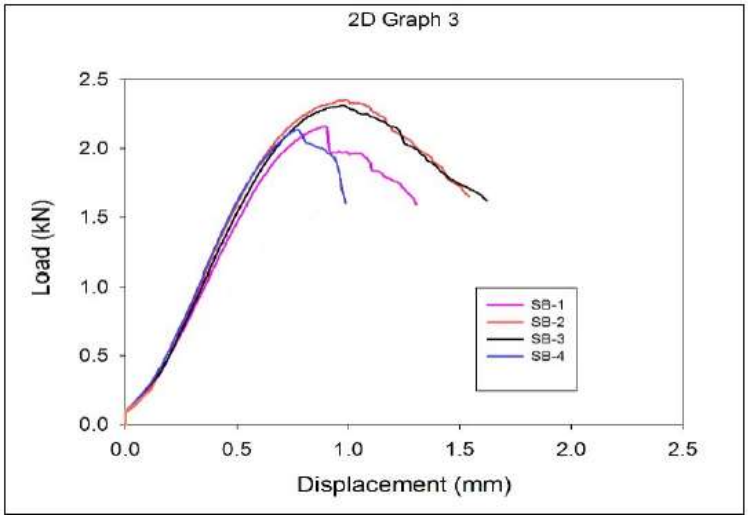

Fig.12: Load-displacement curves

Table 4: Specimen details and experimental results

S. No	Dimensions (mm)	Max. Load (kN)	Strength (MPa)
1	100 x 13 x 11	2.16	11.328
2	100 x 13 x 11	2.35	12.325
3	100 x 13 x 11	2.311	12.120
4	100 x 13 x 11	2.134	11.192
Average		2.238	11.74 ± 1.29

4.2 The results of the compression test

The results of the compression tests, in the form of stress-strain curves, are depicted in Fig. 13 & 14. The tests were conducted along the X and Z directions. From both the figures, it can be perceived that the compression behaviour of 3D PF Cf/C is nearly linear in both the X and Z directions. The material

exhibits a strain to failure of approximately 0.15% in the X direction, with a modulus of 54 GPa. In the Z direction, the material deforms more, showing a strain to failure of around 20% and a modulus of 6.2 GPa. Table 5 compares the compression modulus and strengths obtained from the tests along the X and Z directions

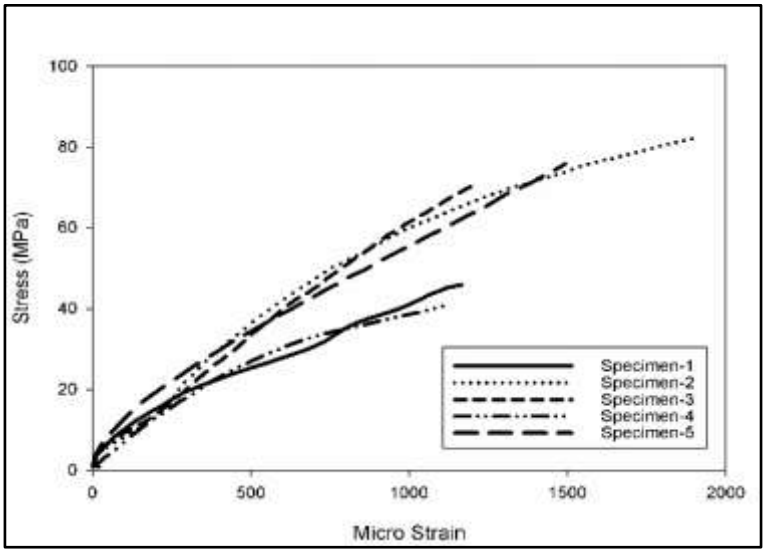

Fig. 13: Stress-strain response under compression along the X Direction

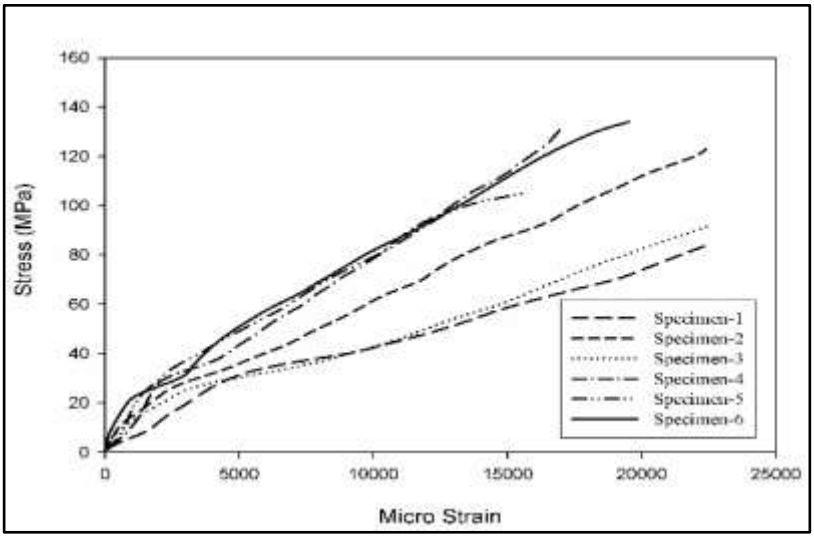

Fig. 14: Stress-strain response under compression along the Z Direction

The results of the compression tests indicate that the Z-direction has superior compressive strength relative to the X-direction. In the X direction, the fabric layers are prone to buckling and instability, which initiates interface debonding and results in premature failure of the composite. In contrast, under Z-direction loading, the fabric layers and the interfaces are subjected to compression, leading to failure at significantly higher loads and resulting in greater composite strength.

The composite exhibits the opposite trend in terms of modulus, with the Z direction having a lower modulus than the X direction. The fiber content in the Z direction is lower, at approximately 5% (contributed by fiber bundles), and the transverse modulus of the fabric layers is also lower, leading to an overall lower modulus in the Z direction. In the X direction, the composite shows a higher modulus because the in-plane modulus of the fibers is very high, but it fails under lower loads due to interface failure.

Industrial Engineering Journal
ISSN: 0970-2555
Volume : 55, Issue 03 : 2026

Table 5: Compression strength and modulus in X and Z directions

Sl. No.	Direction of test	Strength [MPa]	Compression modulus [GPa]
1	X direction	70.9 ± 18	54.2 ± 7
2	Z direction	141 ± 19	6.2 ± 1.7

4.2.1 Tensile test results

The stress-strain curves (Fig.15) obtained from the tensile tests at room temperature in the X-direction show a predominantly linear elastic response up to failure, indicating the brittle nature of the 3D PF C/C composite. All specimens exhibited an approximately linear increase in stress with strain, followed by sudden fracture without significant plastic deformation. The ultimate tensile strength varied among the specimens, with the maximum value reaching about 115 MPa, while the lowest strength was approximately 57 MPa. Similarly, the failure strain ranged from about 0.0011 to 0.0016, indicating some scatter in the tensile behaviour. This variation can be attributed to the heterogeneous microstructure of the composite, including local differences in fibre distribution, matrix density, porosity, and fibre- matrix interfacial bonding. Despite the observed scatter, the overall response demonstrates good tensile load- carrying capability along the X direction, where the fibre reinforcement is dominant. The abrupt failure observed in all specimens confirms that fracture occurs primarily through fibre breakage and matrix cracking, which are typical failure mechanism in carbon-carbon composites under tensile loading.

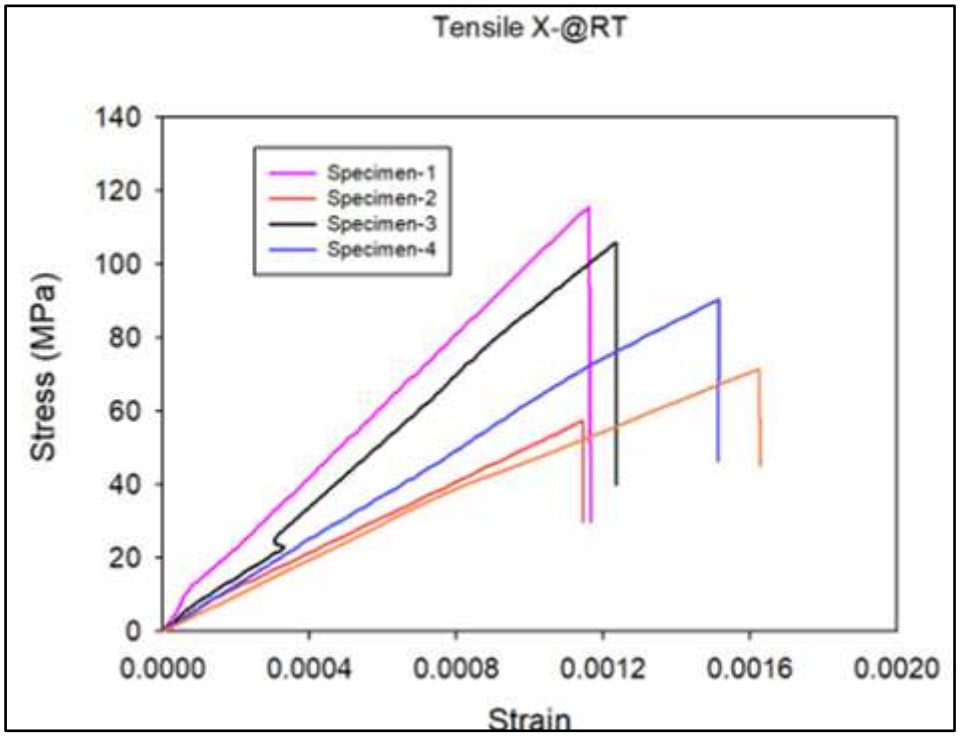

Fig.15: Stress-strain curves for Tension at room temperature in X Direction

The stress-strain curve (Fig. 16) obtained from the tensile tests in the Z-direction at room temperature indicate significantly lower strength and stiffness compared to those observed in the X direction. Both

specimens exhibited an initial elastic response, followed by gradual nonlinear behaviour before failure. The maximum tensile stress attained was approximately 25 MPa for specimen-1 and 15 MPa for specimen-2, demonstrating considerable scatter in the tensile properties. The failure strain ranged from about 0.0005 to 0.0011, indicating limited deformation prior to fracture. The relatively low tensile strength is attributed to the lower fibre content and reduced reinforcement efficiency in the Z direction, where the load is carried primarily by the matrix and through-thickness fibres. The variation between the specimens may be due to local differences in fibre distribution, porosity, and fibre-matrix bonding. Overall, the results confirm that the Z-direction is the weakest orientation of the 3D PF C/C composite under tensile loading, exhibiting lower load-carrying capacity and earlier failure compared to the in-plane direction.

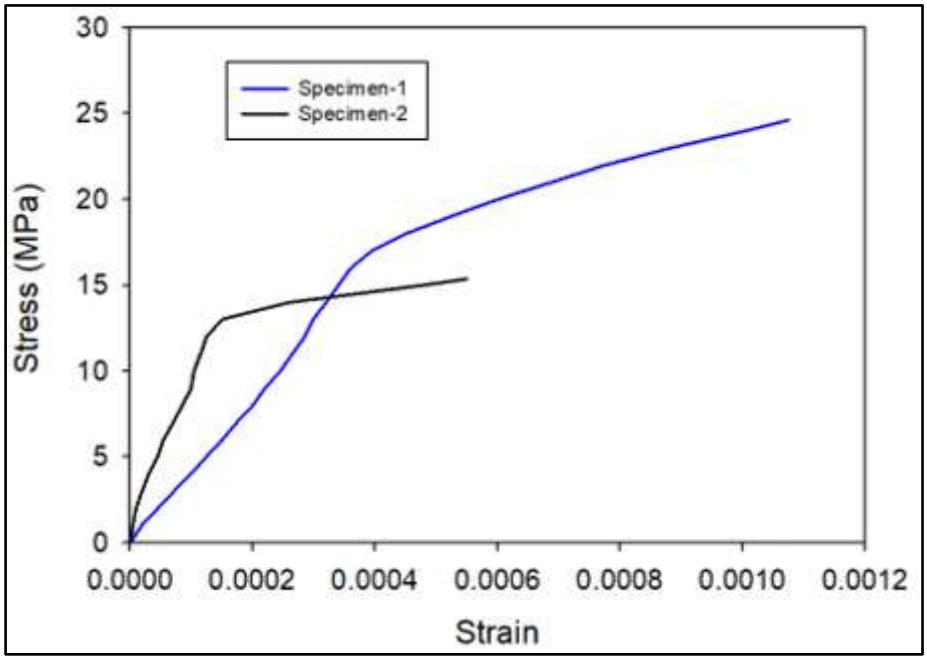

Fig.16: Stress-strain curves for Tension at room temperature in Z Direction

V. Conclusions

- The 3D pierced fabric (PF) C/C composite exhibited anisotropic mechanical behaviour, with properties strongly dependent on the reinforcement direction due to a higher fibre volume fraction in the X–Y plane (25%) than in the Z-direction (5%).
- The Short Beam Shear (SBS) tests showed consistent load-displacement responses and progressive failure behaviour. The average interlaminar shear strength was 11.74 ± 1.29 MPa, indicating adequate through-thickness bonding provided by the pierced-fabric architecture.
- Compression tests revealed significant directional dependence. The Z-direction exhibited nearly twice the compressive strength (141 ± 19 MPa) as the X-direction (70.9 ± 18 MPa) because through-thickness loading suppresses layer buckling and interface debonding.
- The compression modulus showed the opposite trend, with the X-direction modulus (54.2 ± 7 GPa) being substantially higher than the Z-direction modulus (6.2 ± 1.7 GPa) owing to the greater in-plane fibre reinforcement.
- Tensile tests in the X-direction demonstrated a predominantly linear elastic response and brittle fracture behaviour. The composite exhibited good load-carrying capability along the fibre-dominated direction, with tensile strengths reaching approximately 115 MPa

References

[1] Guo, Fei, Xueli Zhang, Ming Qiu, and Longmiao Chen. "Strain-rate-dependent interlaminar shear properties of 3D FWP-C/C composites." *International Journal of Mechanical Sciences* 301 (2025): 110523.

[2] Scarponi, C. "Carbon–carbon composites in aerospace engineering." In *Advanced Composite Materials for Aerospace Engineering*, pp. 385-412. Woodhead Publishing, 2016.

[3] Fang, Zhongwei, Yang Tao, and Diantang Zhang. "Bending mechanical properties and failure mechanism of spreading fabric/felt needled C/C laminated composites." *Composite Structures* 361 (2025): 119047.

[4] Li, Jian, Penglei Guo, Chenglong Hu, Shengyang Pang, Jian Ma, Rida Zhao, Sufang Tang, and Hui-Ming Cheng. "Fabrication of large aerogel-like carbon/carbon composites with excellent load-bearing capacity and thermal-insulating performance at 1800° C." *ACS nano* 16, no. 4 (2022): 6565-6577.

[5] Chen, Xiaoming, Li Chen, Chunyan Zhang, Leilei Song, and Diantang Zhang. "Three-dimensional needle-punching for composites–A review." *Composites Part A: Applied science and manufacturing* 85 (2016): 12-30.

[6] Siron, O., and J. Lamon. "Damage and failure mechanisms of a3-directional carbon/carbon composite under uniaxial tensile and shear loads." *Acta materialia* 46, no. 18 (1998): 6631-6643.

[7] Aly-Hassan, Mohamed S., Hiroshi Hatta, Shuichi Wakayama, Mitsuhiro Watanabe, and Kiyoshi Miyagawa. "Comparison of 2D and 3D carbon/carbon composites with respect to damage and fracture resistance." *Carbon* 41, no. 5 (2003): 1069-1078.

[8] Ramaguru, Guruswamy, Atul Ramesh Bhagat, and Konapalli Saraswathamma. "Compression and Shear Response of 3D Pierced Fabric Cf/C Composite." *Nano Hybrids and Composites* 51 (2026): 13-24.

[9] Li, Dian-sen, Gan Luo, Qian-qian Yao, Nan Jiang, and Lei Jiang. "High temperature compression properties and failure mechanism of 3D needle-punched carbon/carbon composites." *Materials Science and Engineering: A* 621 (2015): 105-110.

[10] Zhang, Yiming, Mingming Yu, Lin Fang, Liying Zhang, Wang Xie, Musu Ren, Pibo Ma, and Jinliang Sun. "Unraveling the effects of preform structures on the microstructure, electromagnetic shielding properties, and thermal conductivity of 3D orthogonal C/C composites." *Journal of Industrial Textiles* 54 (2024): 15280837241230235.

[11] Davies, Ian J., and Rees D. Rawlings. "Mechanical properties in compression of CVI-densified porous carbon/carbon composite." *Composites science and technology* 59, no. 1 (1999): 97-104.

[12] Adams, Donald F. "Micro-analysis of the behaviour of a three-dimensionally-reinforced Carbon-Carbon composite material." *Materials Science and Engineering* 23, no. 1 (1976): 55-68.

[13] Bhagat, Atul Ramesh, and Puneet Mahajan. "Characterization and damage evaluation of coal tar pitch carbon matrix used in Carbon/Carbon composites." *Journal of Materials Engineering and Performance* 25 (2016): 3904-3911.